

Ridge and field tile aerodynamics for a low-rise building: a full-scale study

Amanuel Teclé¹, Girma T. Bitsuamlak^{*2}, Nakin Suskawang³, Arindam Gan Chowdury³
and Serge Fuez¹

¹Laboratory for Wind Engineering Research (LWER), International Hurricane Research Center (IHRC)
/Department of Civil and Environmental Engineering (CEE), Florida International University (FIU), Miami,
Florida 33174, USA

²WindEEE Research Institute, Western University, London, On, Canada

³LWER, IHRC/CEE, FIU, Miami, Florida 33174, USA

(Received June 27, 2011, Revised April 13, 2012, Accepted April 24, 2012)

Abstract. Recent major post-hurricane damage assessments in the United States have reported that the most common damages result from the loss of building roof coverings and subsequent wind driven rain intrusion. In an effort to look further into this problem, this paper presents a full-scale (Wall of Wind --WoW--) investigation of external and underneath wind pressures on roof tiles installed on a low-rise building model with various gable roofs. The optimal dimensions for the low-rise building that was tested with the WOW are 2.74 m (9 ft) long, 2.13 m (7 ft) wide, and 2.13 m (7 ft) high. The building is tested with interchangeable gable roofs at three different slopes (2:12; 5:12 and 7:12). The field tiles of these gable roofs are considered with three different tile profiles namely high (HP), medium (MP), and low profiles (LP) in accordance with Florida practice. For the ridge, two different types namely rounded and three-sided tiles were considered. The effect of weather block on the “underneath” pressure that develops between the tiles and the roof deck was also examined. These tests revealed the following: high pressure coefficients for the ridge tile compared to the field tiles, including those located at the corners; considerably higher pressure on the gable end ridge tiles compared to ridge tiles at the middle of the ridge line; and marginally higher pressure on barrel type tiles compared to the three-sided ridge tiles. The weather blocking of clay tiles, while useful in preventing water intrusion, it doesn't have significant effect on the wind loads of the field tiles. The case with weather blocking produces positive mean underneath pressure on the field tiles on the windward side thus reducing the net pressures on the windward surface of the roof. On the leeward side, reductions in net pressure to a non-significant level were observed due to the opposite direction of the internal and external pressures. The effect of the weather blocking on the external pressure on the ridge tile was negligible.

Keywords: full-scale; ridge tiles; field tiles; tile profile; wind pressure; turbulence; mitigation; low-rise building; underneath pressure

1. Introduction

*Corresponding author, Ph. D., E-mail: gbitsuam@UWO.ca, bitsuamg@fiu.edu



Fig. 1 Damage to roof hip and ridge tiles: (a) Hurricane Charley (FEMA 2005), (b) and (c) Hurricane Ike (IHBS 2009)

Hurricanes have often caused extensive economic losses and human fatalities in communities along their path (Hooke 2007). On the other hand, over the last 50 years America's coastal regions have experienced significant growth in population and infrastructure development, making these areas more vulnerable to hurricane. The losses have increased from \$1.3B/yr pre-1990 to \$36B/yr post-2000 (Rappaport 2000) with 1,400 fatalities in 2004-05 (Cutter *et al.* 2007) and losses exceeding \$100B (Lott and Ross 2006) in 2005 alone. Even though a number of mitigation techniques have been introduced to improve the performance of building envelopes, the damage to roofs and roof components is still the major cause of building performances during hurricanes (FEMA 2005). For instance, a team deployed by IBHS reported a pattern of failure from Hurricane Ike (80-90 mph) "Aerial photos taken after Ike showed close to 90 percent of the homes near the coast toward the western part of Bolivar Peninsula had an extensive loss of hip and ridge shingles" (IBHS 2009). Among the different pattern of wind-induced damages to building envelopes, wind damage initiated at roof corners, edges, ridges and hips appears to be the most dominant cause for frequent loss occurrences as reported in FM (1985), IBHS (1999a, 1999b, 2009), FEMA (2004) and FEMA (2007).

Because of vortex formation, the uplift forces are excessive at the corners of the roof. The corner roof vortices often generate extreme suction pressures along the leading edges. The severity of vortex-induced uplift observed on roofs is well documented by the following researchers (Stathopoulos 1987, Kramer and Gerhardt 1989, Saathoff and Melbourne 1989, Stathopoulos *et al.* 1990, Cochran and Cermak 1992, Gerhardt and Kramer 1992, Mehta and Levitan 1992, Cochran *et al.* 1993, Tieleman *et al.* 1994, Lin *et al.* 1995, Kawai and Nishimura 1996, Lin and Surry 1998, Banks and Meroney 2001, Robertson *et al.* 2007). Once the roof corner is ripped off, the damage usually cascades to other areas and cause subsequent damage due to water intrusion, change in internal aerodynamics, etc. Research have shown that immediately after the first roof panel has been removed by wind uplift, the magnitude of losses could be in the range of 80% of the total insurance claims (Sparks *et al.* 1994).

A significant effort has been made to address these interrelated issues. For example, widespread hurricane damage to hip and ridge tiles resulted in the development of an intensive set of guidelines for hip and ridge tile installation, which was adopted into the Florida Building Code (FBC) as provided in section 1507.3 of the code. The FBC regulation for installation of clay and concrete roof tiles is in compliance with the recommendation of the Florida Roofing, Sheet Metal

and Air Conditioning Contractors Association (FRA) and the Tile Roofing Institute (TRI). These code recommendations are prescriptive in nature and more research is needed to relate the recommended installation details with the expected magnitude of wind pressures on different roof slopes, ridge types, and wind angles of attack etc. Industry approved testing protocols, such as FM 4470, ASTM E1592, and UL 1897 are used to investigate the uplift resistance of roofing materials statically by applying pneumatic pressure. To this effect, a group of researchers recently evaluated the resistance of hip and ridge tiles through a detailed experimental and analytical study for clay and concrete tiles with adhesive-set, mortar-set as well as mechanical attachments by using static tests on a single clay tile (Mirmiran 2006, Mirmiran *et al.* 2007, Huang *et al.* 2009). A further study was performed using monotonic and cyclic uplift tests for multiple clay tiles (three at a time), as well as dynamic wind simulation tests using a 2-fan Wall of Wind (WoW) apparatus on small mono-slope roof specimens that have clay field tiles (Huang *et al.* 2009). Their study was limited to mono-slope tests because of the limitation of the wind field size generated by the 2-fan WoW.

This paper presents an investigation of the aerodynamic performance of roof tiles (both ridge and field tiles) installed on gable roofs with three different slopes (i.e. 7:12, 5:12, and 2:12), three different field tile profiles (i.e. high, medium and low) and two types of ridge tiles (barrel and three sided), with each experiment being performed under weather block (WB) and no weather block (NWB) conditions. The new 6-fan WoW facility at Florida International University (FIU) was used to test these buildings. This 6-fan WoW is 4.88 m (16 ft) high and 7.31 m (24 ft) wide and is capable of testing a large low-rise building model. The performance of the roof tiles under different wind angles of attack (AoA) is studied to capture the critical wind loading that may lead to roof failure. In order to evaluate the net pressure on the roof tiles, the distribution of external pressure on the top surface of the tiles as well as the “internal” pressure underneath the tiles (i.e. between tile and roof deck) was measured and analyzed. The aim was to measure the “internal” pressure that may develop underneath the field tiles due to porosity and the discontinuous nature of the roof system. In addition, the effect of weather blocking was investigated to understand its influence on the aerodynamic performance of the field and ridge tiles. This study generated high resolution aerodynamic data for field and ridge tiles installed on roofs with different slopes and tile profiles as well as using different construction details that will provide for useful insight to the failure mechanism of roof components as described in the following sections.

2. Methodology

The present study has adopted a full-scale experiment using the WoW testing facility aimed at acquiring high resolution aerodynamic data for gable roof ridges and field tiles. The WoW testing facility involves the experimental setup of larger size models that are assembled with industry standard construction materials that create a direct resemblance to actual wind-to-tile interactions. However, testing larger specimens within the finite WoW wind field, either to produce larger Reynold's number flows or to assess the performance of full-scale building components, may entail blockage issues. The concerning blockage effect in this experiment is the size of the test specimen in relation to the size of the wind field generated by the WoW at the inlet. The initial model size of the test building specimen was obtained through a computational blockage and proximity assessment simulation in the Wall of Wind (Bitsuamlak *et al.* 2009). Based on the experimental result of that simulation a 2.13 m (7 ft) dimension was chosen for the depth and height of the model. The width of the building was chosen to be 2.74 m (9 ft) so that the test



Fig. 2 Test specimen in front of Wall of Wind at 0° AoA

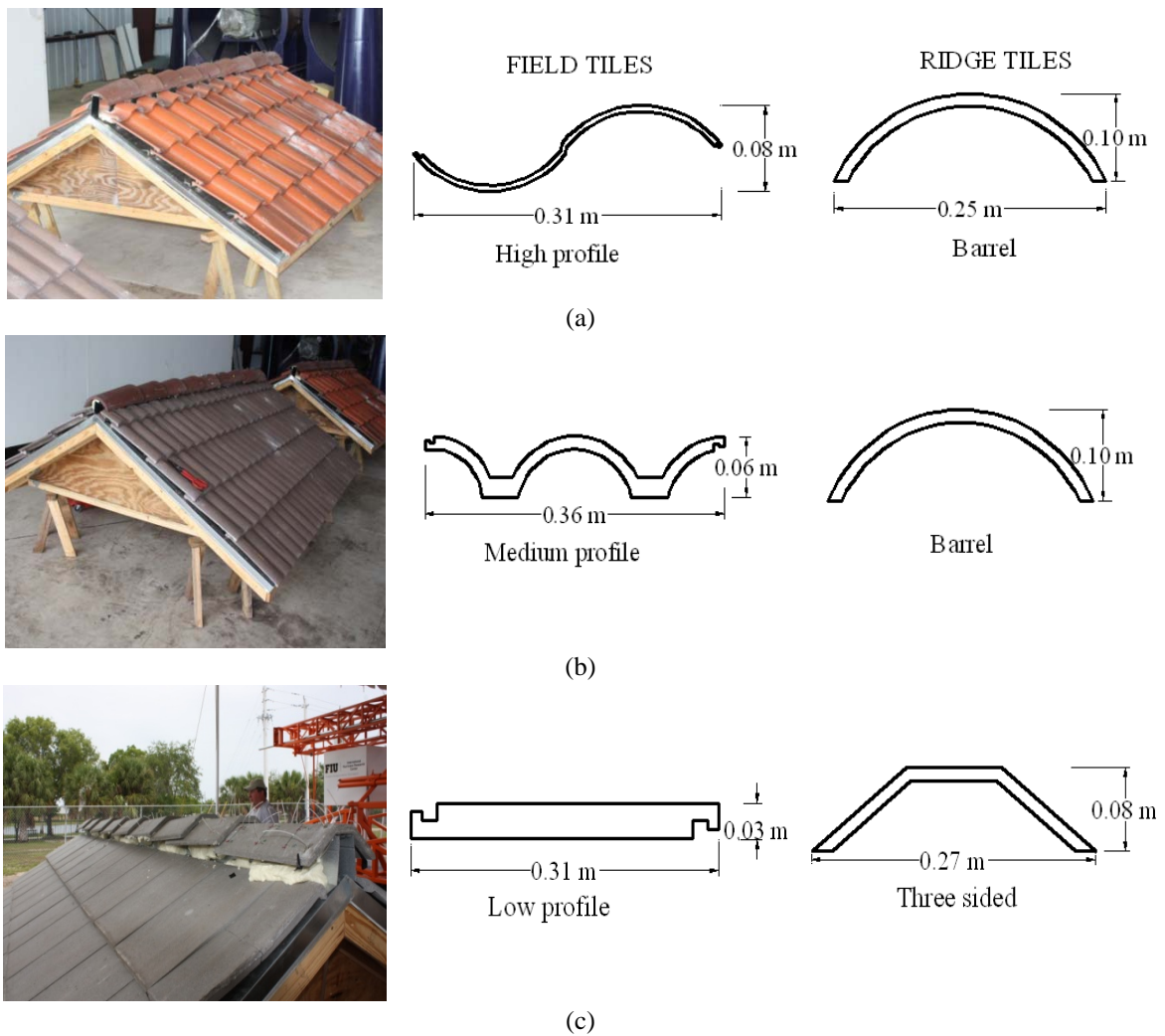


Fig. 3 Field and ridge tile combinations: (a) high profile field with barrel ridge tiles, (b) Medium profile field with barrel ridge tiles and (c) Low profile field with three sided ridge tiles

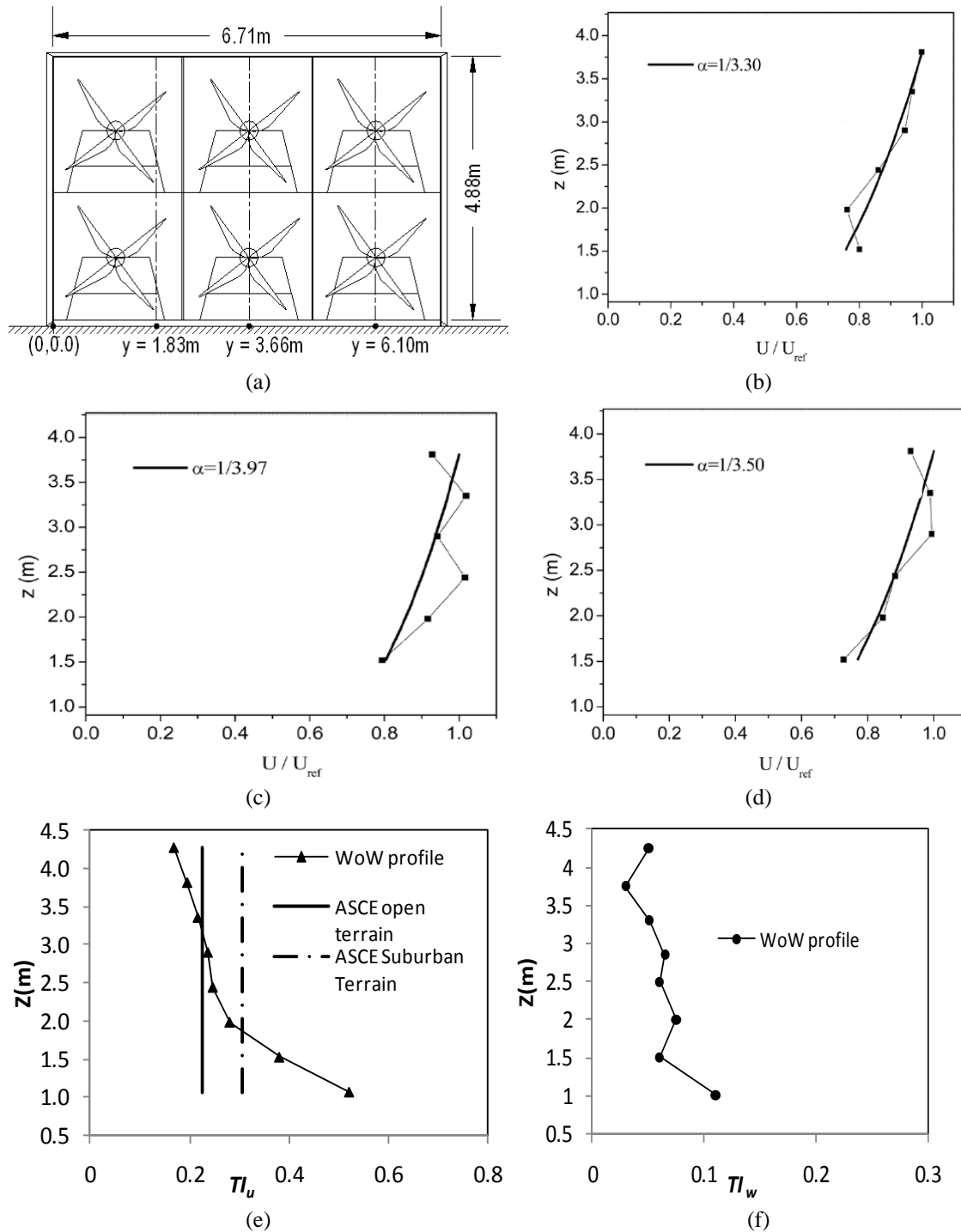
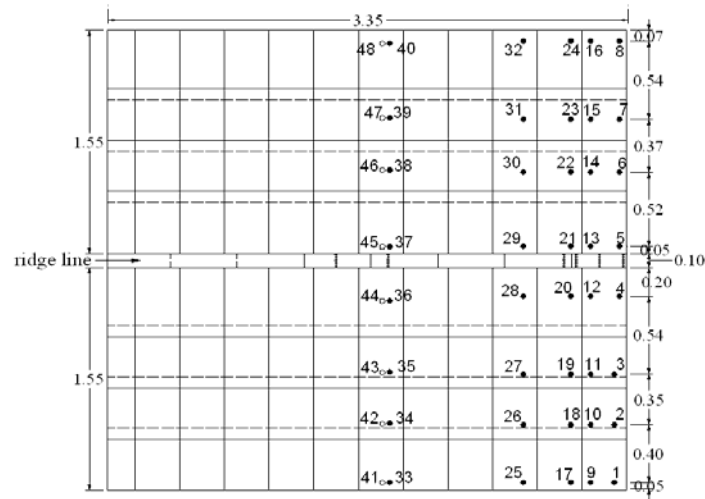


Fig. 4 Full-scale 6-fan WoW: (a) non-dimensional mean velocity profiles at $y = 1.22\text{ m}$ --4 ft--, (b) at $y = 3.66\text{ m}$ -- 12 ft --, (c) at $y = 4.27\text{ m}$ -- 14 ft --, (d) longitudinal, (e) vertical turbulence profile and (f) at $y = 3.66\text{ m}$ (12 ft)



(a)



(b)

Fig. 5 Pressure tap distribution on the field tiles (plan view): (a) tap layout and (b) tap placement

building would have a representative rectangular foot print as shown in Fig. 2. Following Florida’s building code of practice, barrel ridge tiles were used with high and medium field tiles and three-sided ridge tiles were used for the low profile field tiles. All field and ridge tiles used in this study are schematically shown in Figs. 3(a) to 3(c). While the field tiles were nailed to the roof deck, the ridge tiles were attached to a metal channel by using adhesive foams. Since the present WoW experiment is purely an aerodynamic study (dealing with shapes, porosity or openings and their interaction with wind), adhesive foams were used for the weather blocking instead of mortar due to their ease of application and reuse of the model.

A mean wind speed of 22.3 m/s (49.79 mph) and turbulence intensity of 22% measured at an eave height of 2.18 m (7.16 ft) from the ground was used. A 3-minute wind speed was recorded in

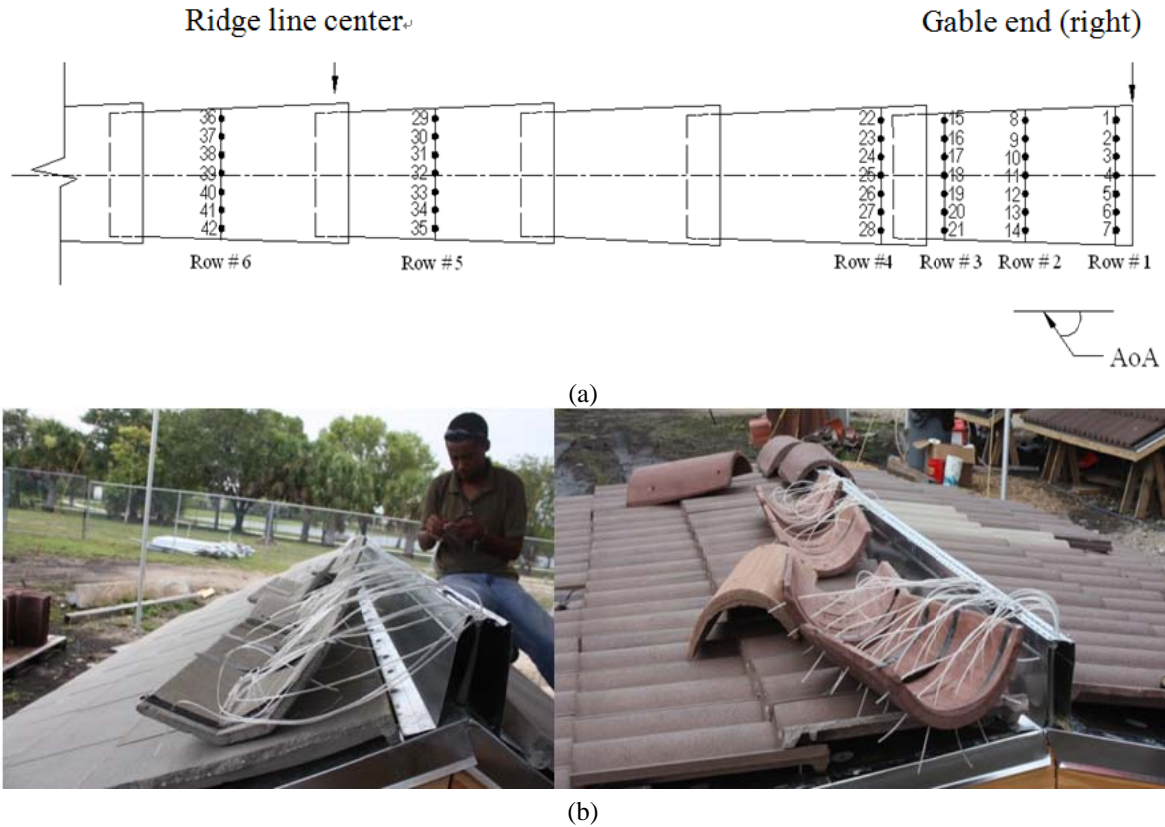


Fig. 6 Ridge tile Pressure tap distributions: Pressure tap layout along ridge line

the absence of the model building for use as a reference wind speed. The reference mean wind speed was obtained by averaging three cobra probe measurements. The probes were equally spaced, coinciding along the front eave line of the building. The mean wind speed and turbulence intensity profiles are shown in Figs. 4(a) to 4(f). For more details on the wind flow generation methods, refer (Huang *et al.* 2009). As can be seen in the wind profile plots, the wind profile is not as smooth as expected in a standard wind tunnel wind field. However, the larger wind field and higher wind speed provide for useful insight into the tile aerodynamics that might not have been possible in a standard wind tunnel tests.

A total of ninety four pressure taps were installed on each gable roof to capture the external pressure distribution on the tiles and the internal pressure developing in the space between the tiles and the roof deck. SETRA low pressure differential transducers (model 265) were used. Each transducer is supplied with two factory-installed $\frac{1}{4}$ " (outside diameter) pressure ports: a reference (low) pressure port and a positive (high) pressure port. At the WoW, the underground pit where the reference pressure is measured was located approximately 15 m to one side of the WoW and was outside the wind field generated by the WoW. The positive (high) pressure ports measure the fluctuating pressure at a specified location of interest. Forty eight SETRA transducers were used on the field tiles whose distribution is shown in Fig. 5. The remaining forty six transducers were used on the ridge tiles whose distribution is shown in Fig. 6. Six rows of pressure taps were placed

on the external surface of the ridge tiles, each row having seven taps (Figs. 6(a) and 6(b)). For high spatial resolution pressure measurements, a total of 21 transducers were allocated for the edge ridge tile. Four pressure taps were installed on the ridge support to capture any internal pressure developing underneath the ridge tiles. Eight pressure taps at the center, perpendicular to the ridge of the building, were also installed between the field tiles and the roof deck (Fig. 5). In order to keep the accuracy of the measurements and avoid the uncertainty that arise from wiring, the pressure transducers were calibrated each time a new set of tests were performed. Reference pressures were taken twice for each test: before and after test and eventually the mean of the two was taken in the analysis. The pressure signals from all taps were sampled at a rate of 100 Hz for 180 seconds.

Each of the six gable roofs were tested for five different wind angles of attack (AoA) ($\alpha = 0^\circ, 30^\circ, 45^\circ, 75^\circ, \text{ and } 90^\circ$). The 0° wind AoA corresponds to the orientation of the building when the gable-end is facing the windward wall (as shown in Fig. 2). The AoA increases as the building rotates counterclockwise. Once the tests without weather blocking were completed, the weather block was applied and the tests were repeated to assess the effect of the weather blocking.

3. Results and discussions

The non-dimensional pressure coefficient for each tap on the building was calculated by referencing all measured pressures to the mean free stream dynamic pressure as

$$C_{pej} = \frac{P_{ej} - P_{rj}}{\frac{1}{2} \rho V^2} \quad (1)$$

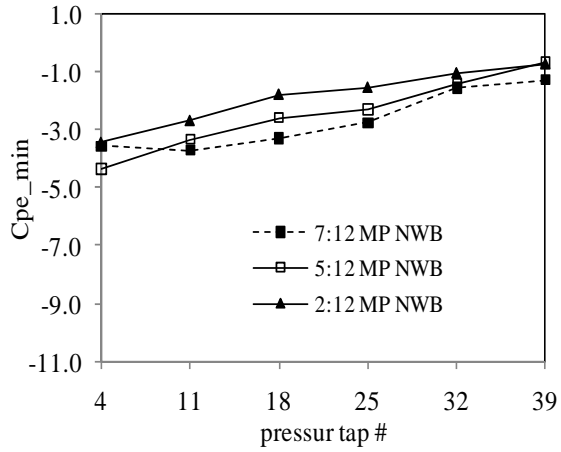
$$C_{pij} = \frac{P_{ij} - P_{rj}}{\frac{1}{2} \rho V^2} \quad (2)$$

Where C_{pej} is computed external pressure coefficient; C_{pij} is computed internal pressure coefficient, P_{ej} and P_{ij} are the measured external and internal fluctuating pressures, respectively at the j^{th} tap; P_{rj} is the average reference pressure taken before and after the test; ρ is air density (taken as 1.1644 Kg/m^3 taken at 85°F average temperature); V is the mean reference wind speed. The mean pressure coefficient for each tap is obtained by taking the average of the 3 minute recorded differential pressure

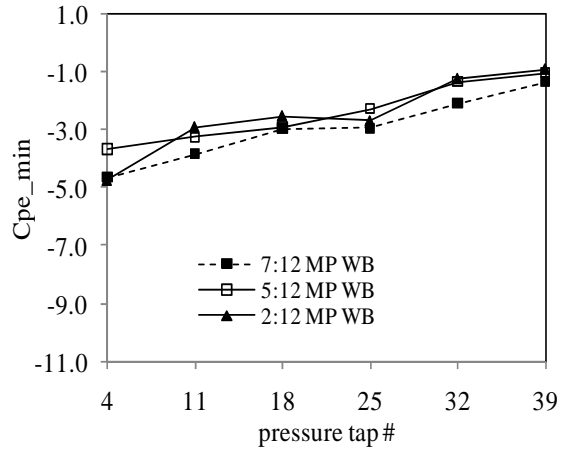
$$C_{pmean} = \frac{1}{n} \sum_{i=1}^n C_{pi} \quad (3)$$

Similarly, the peak positive and suction pressure coefficients are obtained from the time history data as

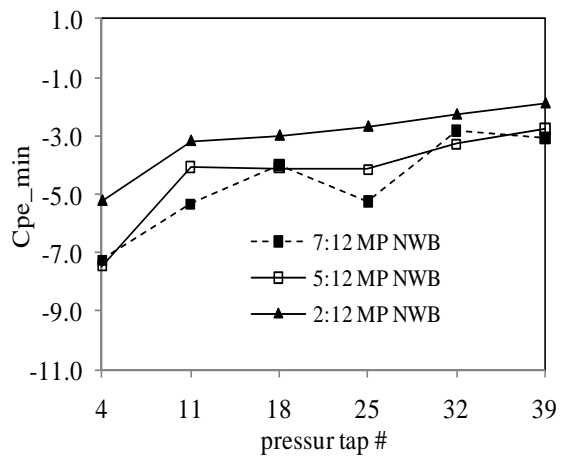
$$\hat{C}_{pi} = \frac{\hat{P}_{ij} - P_{rj}}{\frac{1}{2} \rho V^2} \quad (4)$$



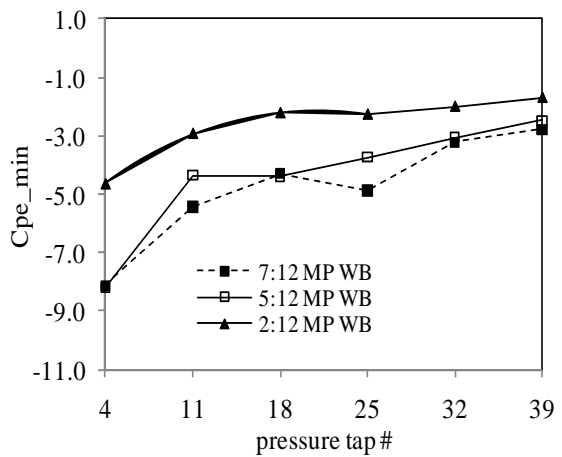
(a) 0° AoA NWB barrel ridge tile



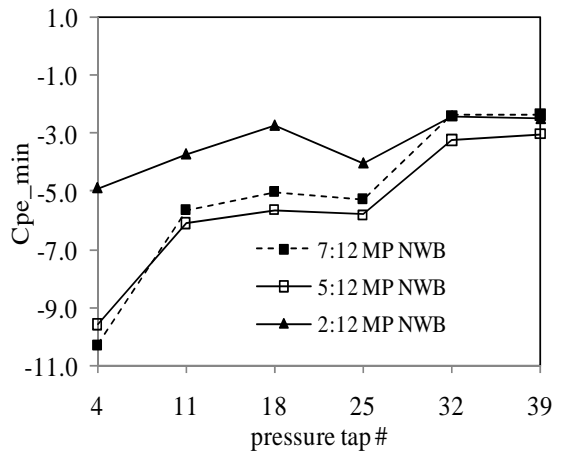
(b) 0° AoA WB barrel ridge tile



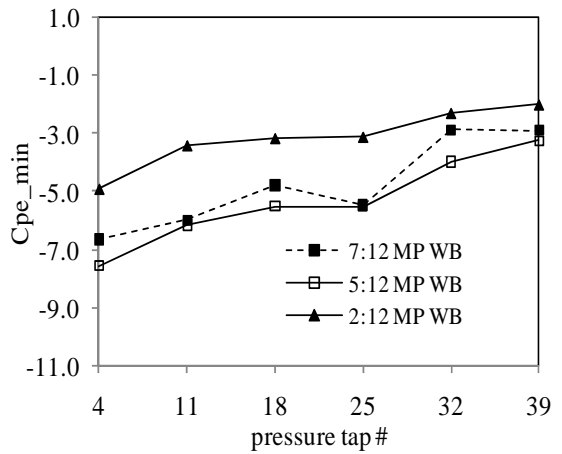
(c) 30° AoA NWB barrel ridge tile



(d) 30° AoA WB barrel ridge tile



(e) 45° AoA NWB barrel ridge tile



(f) 45° AoA WB barrel ridge tile

Fig. 7 Pressure distribution along the crest of the ridge tiles

$$\tilde{C}_{pi} = \frac{\tilde{P}_{ij} - P_{rj}}{\frac{1}{2} \rho V^2} \quad (5)$$

Where \hat{P}_i is the peak fluctuating pressure.

The mean root square value of the pressure coefficient is obtained by making use of the standard deviation of the pressure coefficient as

$$\tilde{C}_{pi} = \sqrt{\frac{1}{n} \sum_{i=1}^n (C_{pi} - C_{pmean})^2} \quad (6)$$

Different parametric analyses were conducted as discussed below.

3.1 Pressure distribution along ridge tile

The external pressure coefficient distribution over the surface of the ridge tile was evaluated for the three roof slopes with medium profile (MP) along the length of the ridge line spanning from the gable-end to the center of the ridge line. As shown in Fig. 6(a), six rows of pressure taps across the ridge line were used. The pressure taps at the crest of the ridge were selected for the discussion on the pressure distribution along the ridge line (i.e. tap #4, 11, 18, 25, 32 & 39). In most cases, the ridge tiles experience the worst separated flows at their crest as observed during the experiment. For this particular discussion 0° AoA and the worst AoA cases (i.e. 30° and 45° AoA) are considered. As illustrated in Figs. 7(a)-7(f), it was observed that critical suction pressure occurred at the edge of the gable-end ridge tile. Pressure taps at row #1 experienced the maximum suction pressure both at 30° and 45° AoA for all roof slopes tested under both the WB and NWB conditions. This is mainly attributed to the onset of a conical vortex and separation bubble at this particular region for the specified wind angle of attack. Moving from the windward edge to the mid section (i.e. from row #1 to row #6), a significant reduction in suction pressure (i.e. a reduction of $C_{p_{min}}$ from -9 to -3) was observed. It was observed that the roof slope 2:12 experiences comparatively a very mild suction pressure at the gable-end ridge tile and the 7:12 slope experience the highest suction in most of the cases observed in the present study (as shown in Fig. 7(e)). The difference on the suction pressure among the three roof slopes disappears while moving from the gable-end to the middle of the ridge line (as shown in all Figs. 7(a) to 7(f)).

3.2 Roof profile effect on field tiles

It was observed that the type of roof tile profile has considerable effect on the pressure distribution that develops on the roof surface. In this case, the 1st and 2nd rows (i.e. parallel to the eave) of pressure taps on the field tiles of the 7:12 slope were considered for comparison as shown in Figs. 8(a) and 8(b). It was observed that the LP roofs experience higher suction pressure compared to that of HP and MP on windward direction. A similar pattern was observed on the pressure distribution along the length (i.e. parallel to the gable end) of the roof as shown in Figs. 8(c) and 8(d). Compared to other slopes, the suction pressure on the leeward side for the steepest slope (i.e. 7:12) was generally high and particularly LP roof tiles experienced comparatively higher suction pressure (as shown for example in Figs. 8(d) taps #5, 6, 7 and 8). In both cases (i.e.

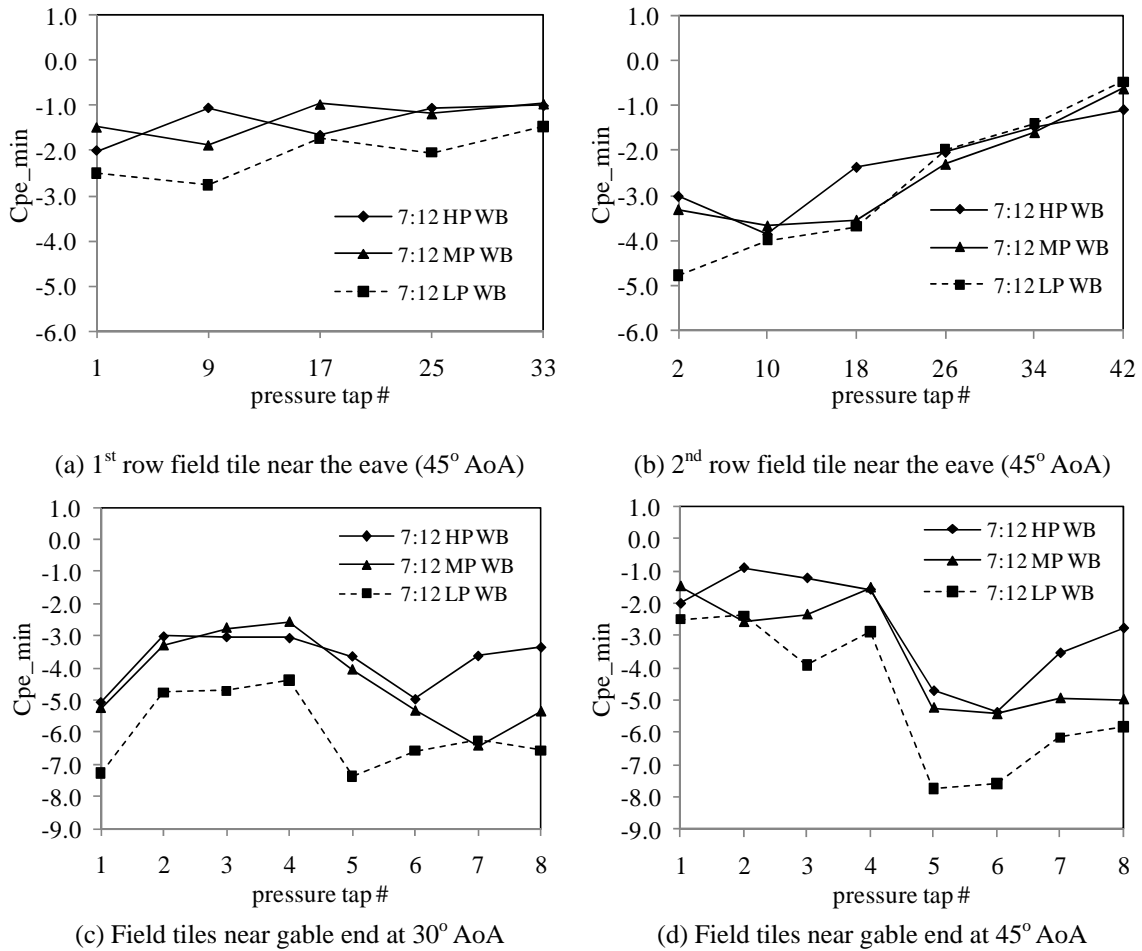


Fig. 8 Field tile profile effect on wind pressure coefficients

both at the edge and on the field surface), it is noticed that the field tile profile has played a significant role on the magnitude and distribution of the wind induced pressure. The LP roof tile being continuously sharp at the edges and monolithically flat on the surface of the roof has resulted in increased flow separation leading to higher suction pressure. On the other hand, the curved edges and rugged surfaces of HP and MP roof tiles have played a role in dampening the flow separation thus resulting in a reduced pressure compared to that of the LP. The wind load reductions on tall buildings due to balconies or chamfering at the corners can be considered analogous to the effect of the tile profile in the present study.

3.3 Field tile profile effect on ridge tiles

The effect of field tile profile (i.e. HP, MP or LP) on the pressure distribution over the surface of ridge tile was investigated as follows. Three rows of pressure taps (i.e. 1st row, 2nd row and 3rd row) from the edge ridge tile (described in Fig. 6(a)) were investigated for this case. These rows

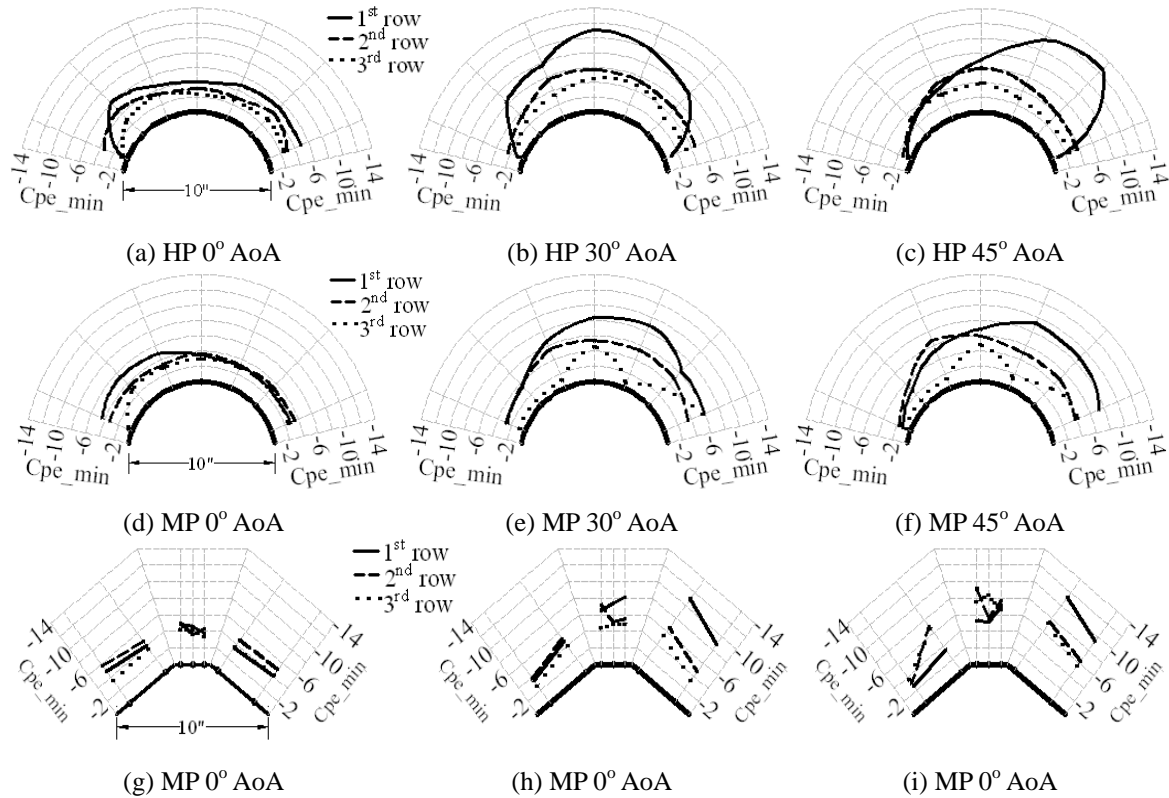


Fig. 9 WB profile effect on ridge tile pressure distribution with roof slope of 7:12

were observed to be the most critical wherein maximum suction was produced due to the flow separation. As illustrated in Fig. 9, the 30° and 45° wind AoA resulted in higher suction pressure compared to the other wind AoA. The coefficients of pressure measured on the 1st row taps (i.e. the outer row closest to the gable end) were higher than that of the inside 2nd and 3rd rows (Figs. 9 and 10). For the 30° AoA, the HP ridge tile experiences high suction pressure as compared to that of the MP (Figs. 9(b) and 9(e)). For the 45° AoA, both HP and MP ridge tiles experience comparable suction pressure on the windward side of the building. However, on the leeward side, the HP ridge tile experiences extremely high suction pressure (Fig. 9(c)). Even if the ridge tile for the LP roof profile is three-sided and cannot be directly compared with that of barrel ridge tiles, it can be observed that the suction pressure is considerably high. Close observation of each ridge tile with respect to the field tile profile provided an insight on the level of flow separation that develops on the ridge. For example, the elevation of the crest of the barrel ridge tile from the valley of the HP field tile is considerably higher than that of the same barrel ridge tile placed on MP field tile because of its higher valley depth. Aerodynamically, the elevated surface of the ridge tile contributes to the formation of higher positive pressure on the windward side of the ridge and higher separation flow on the leeward side (Figs. 9(a) to 9(f)). In the case of the three-sided ridge tile mounted on the LP profile field tile, the higher suction is attributed to the sharp edges of the three sided ridge tile on the crest along with its higher elevation from the roof surface (as can be seen in Fig. 5(c)). Thus, this effect of the field tile profile on the ridge tiles demonstrates that the

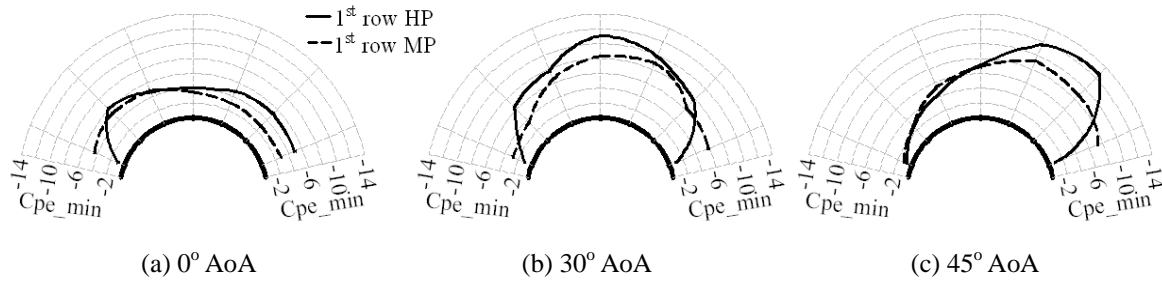


Fig. 10 Field tile profile effect on wind pressure coefficients

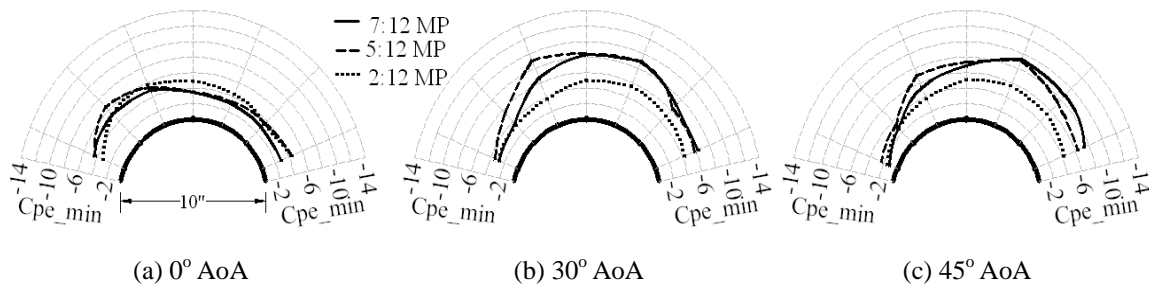


Fig. 11 Slope effect on ridge tiles for the case with weather block and medium profile field tile

higher elevation of ridge tiles due to the overall roof surface profile at a critical wind AoA produces higher wind loading on the ridge tiles.

3.4 Slope effect on ridge tiles

The effect of the slope on the ridge tile pressure distribution was assessed by considering the critically loaded edge ridge tile. As shown in Fig. 9, the first 3 rows of edge tile pressure taps were analyzed for 0°, 30° and 45° wind AoA. The measurement shows that the suction pressure is highest closer to the edge i.e. on the 1st row pressure taps followed by the 2nd and 3rd rows. By considering only the critical row (i.e. 1st row), slope effect comparison was assessed among the three MP roof slopes (Fig. 11). The pressure coefficients for the 0° AoA were within close range of similarity. For the 30° AoA, the 5:12 and 7:12 roof slopes experience relatively higher suction pressure compared to the 2:12 slope. However the 7:12 and 5:12 roof slopes were relatively comparable to each other. For the 30° AoA case, the wind-ward pressure coefficient of the 5:12 slope goes marginally higher than that of 7:12. For the 45° AoA case, however, the leeward pressure coefficient of the 7:12 slope goes marginally higher than that of the 5:12.

3.5 Comparison of edge field tiles vs edge ridge tiles

It is known from previous studies that the suction pressure at the eaves, corners and edges of a roof are the highest. But only a few studies showed high resolution tests that differentiates ridge tiles from field tiles. In the present study, pressure coefficient comparison for the worst case for field tiles versus that of ridge tiles was performed for 7:12, 5:12 and 2:12 roof slopes with WB and

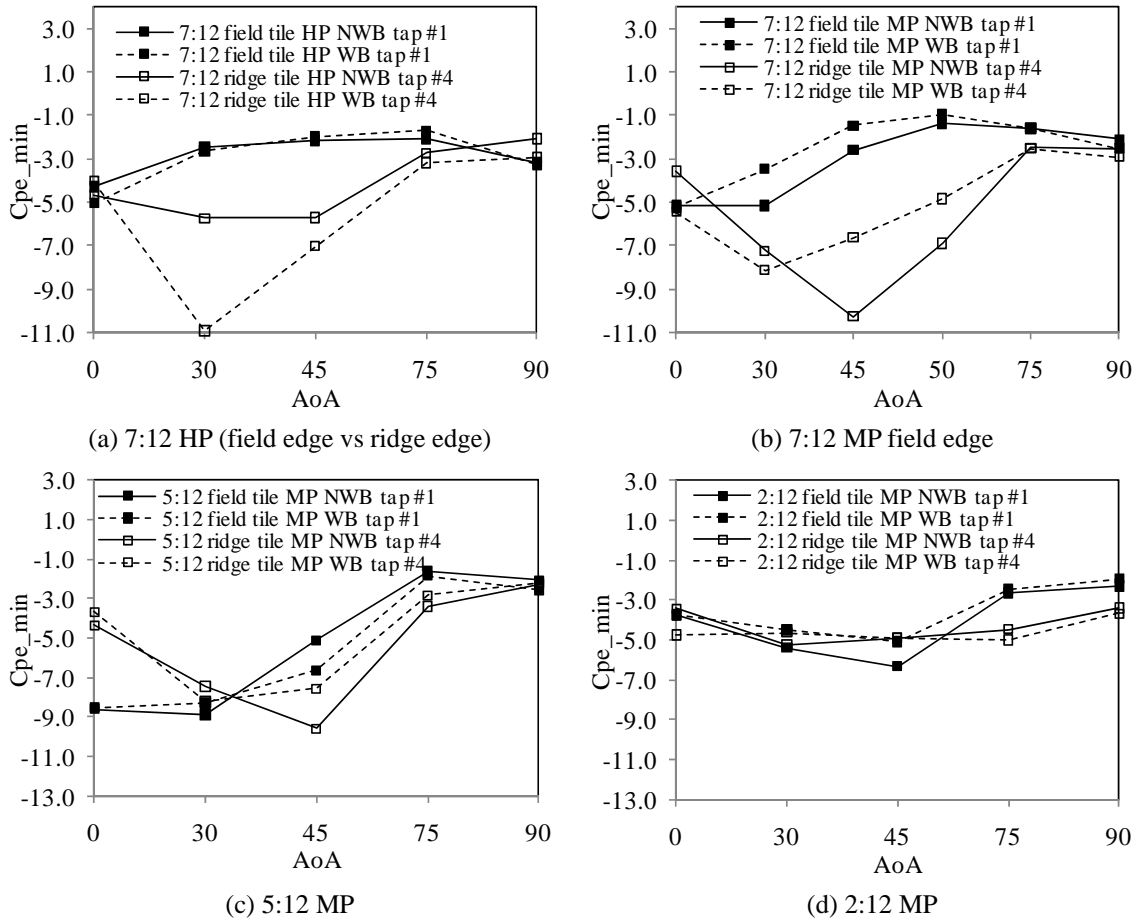


Fig. 12 Edge ridge crest (tap#4) versus corner edge field tile (tap#1) pressure coefficient comparison

NWB conditions. Corner field tile tap #1 (at the eave corner) and edge ridge tile tap #4 (at the crest of gable end) were selected as representative of worst locations for the onset of separation and conical vortices. As illustrated in Figs. 12(a) and 12(b), it was obtained that the edge ridge tile gets exposed to higher suction pressure compared to that of corner edge field tile. The peak suction pressure coefficient on the ridge tile is extremely high for wind angle of attack between 30° and 45°. The $C_{p_{min}}$ for the edge ridge was 180% to 390% higher compared to that of its corresponding corner field tile. The main difference observed between the corner field and ridge tile was the trend of pressure coefficients that both the field and ridge tile experienced with respect to the wind direction. Particularly for oblique wind directions (i.e. 30° and 45° wind AoA) the ridge tile sees significantly higher suction compared to the corner field tile both for WB and NWB cases (Figs. 12(a) to 12(d)).

In another observation, the high resolution data has helped to assess and compare the pressure distribution on the field tile near the ridge with that on the ridge. As shown in Figs. 8(c) and 8(d), the critical suction pressure coefficient on field tile tap #4 (close to the edge ridge line) was obtained to be -4.4. This field tile pressure, however, is much smaller than the nearby ridge surface

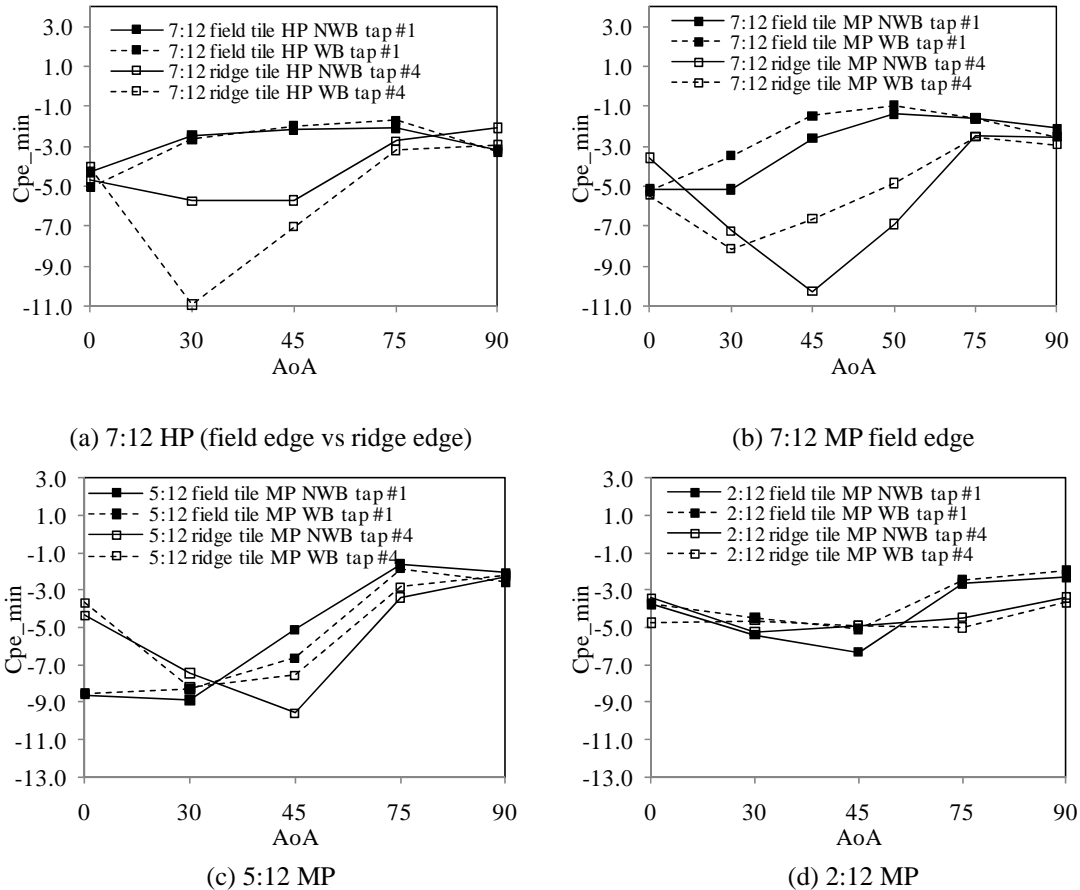


Fig. 13 C_{pi} underneath field tile: (a) 90° AoA NWB_max, (b) 90° AoA WB_max, (c) 90° AoA NWB_mean and (d) 90° AoA WB_mean

pressure as shown in Figs. 9(c), 9(d) and 9(f). The ridge tile pressure was observed to be more or less twice that of the field tile close to the ridge tile.

These differences would not have been captured while testing at small scale such as those carried in a typical wind tunnel. Small scale models do not replicate tile profiles aerodynamically.

3.6 "Internal pressure" underneath field tiles

The discontinuous roof tile system covering the roof deck usually leaves open spaces that allow infiltration/exfiltration of air in between the roof deck and the tiles. Although the openings at the tile over-lap are generally helpful for convective ventilation purposes in order to cool the underlayment (or secondary water barrier), it may also act as a pathway for water intrusion. From the perspective of the present study, however, during extreme wind flows the opening spaces particularly those at the eave and gable end perimeter (here forth called "edge opening") and field tile overlap (here forth called "overlap opening") influences the wind aerodynamics on the roof surface.

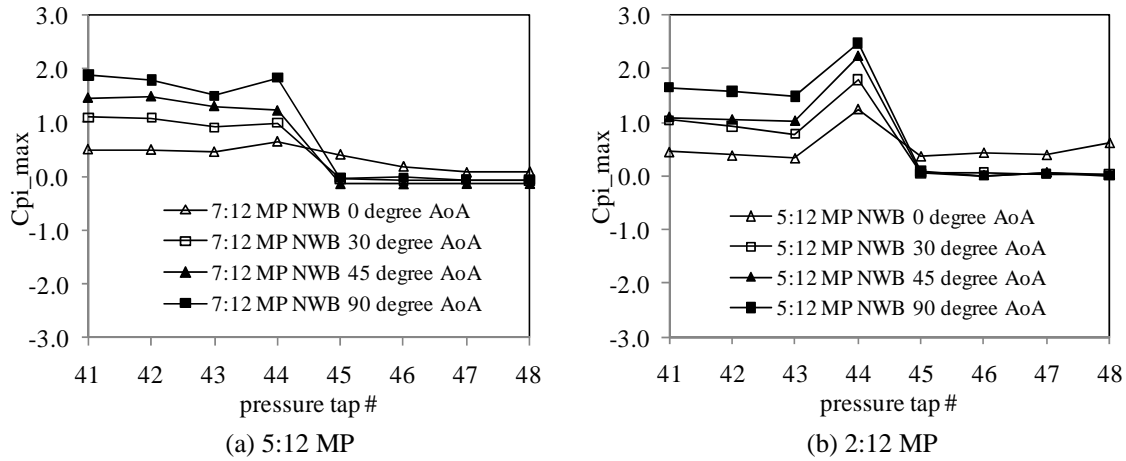


Fig. 14 Max C_{pi} vs wind angle of attack

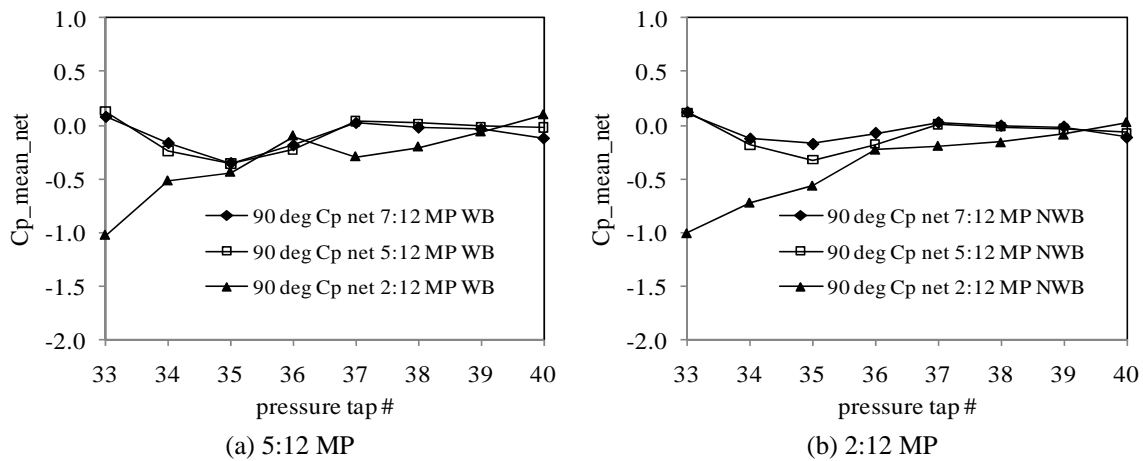


Fig. 15 Comparison net mean roof pressure between weather blocked and non-weather blocked roof tiles

Pressure transducers installed at the roof center line (Fig. 5(a)) along the length of the roof perpendicular to the eave (i.e. tap #41-48 running parallel to the gable end) were used to measure the “internal pressure” underneath field tiles. As shown in Figs. 13(a) and 13(b), the max C_{pi} for the windward edge internal pressure underneath tile (i.e. tap #41-44) was observed to be significant for the 7:12 HP tile profiles. Comparatively, the positive pressure underneath the tiles for MP and LP roof types was moderate. In the MP and LP type of tile profiles, the edge opening between the tile and the roof deck is minimal compared to that of HP roofs wherein which large openings exist. The effect of roof slope on the underneath pressure was studied by comparing the mean C_{pi} for MP of 7:12, 5:12 and 2:12. It was observed that the 7:12 roof type, irrespective of the weather blocking, experience higher positive pressure coefficients (Figs. 13(c) and 13(d)). The steeper the roof slope, the higher the positive pressure underneath the field tiles. Analyzing the peak positive internal pressure coefficient underneath field tiles with respect to the wind AoA, irrespective of the slope of the roof, it was observed that 90° AoA instigates the maximum C_{pi} . The

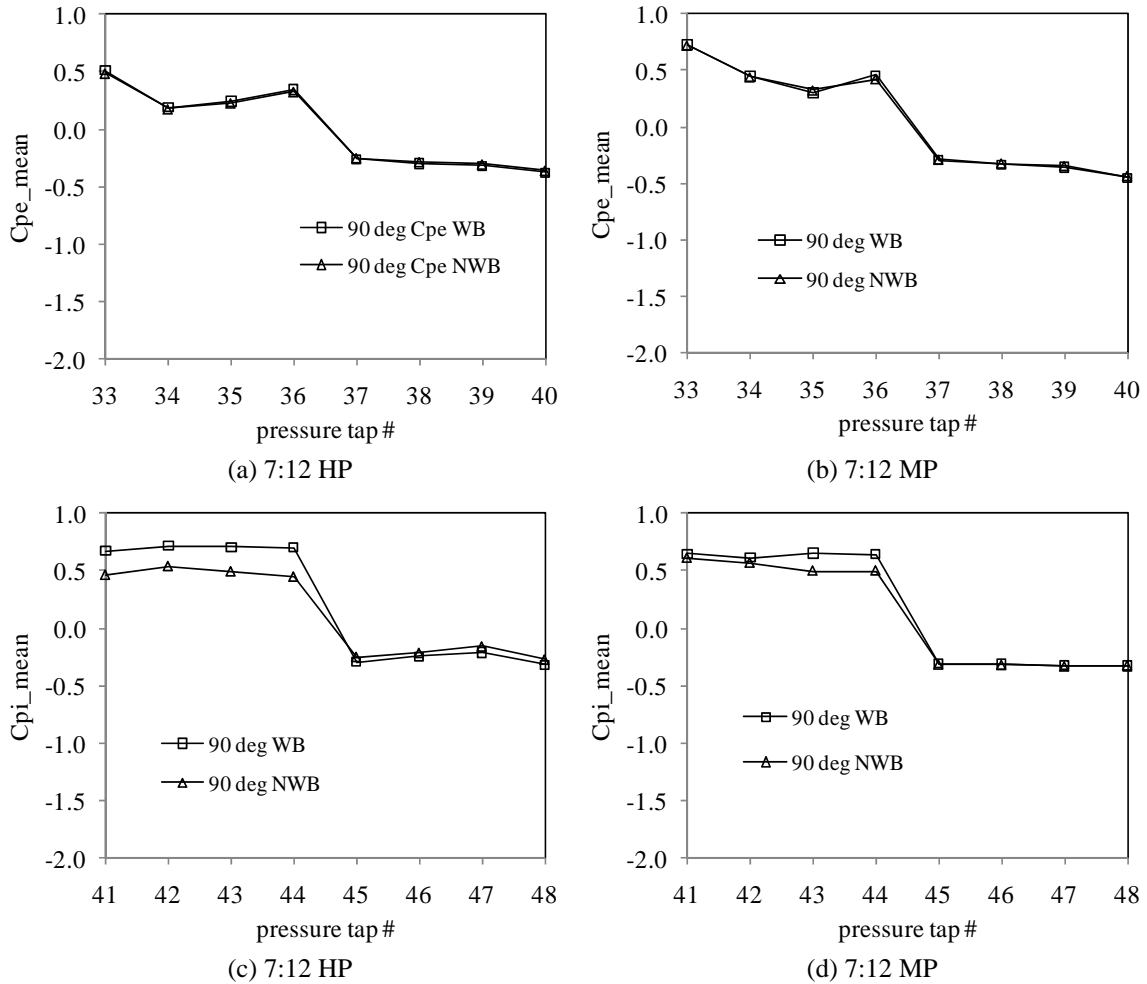


Fig. 16 Comparison between weather blocked and non-weather blocked roof tiles: mean C_{pe} (a) and (b), mean C_{pi} (c) and (d)

lowest was recorded at 0° AoA. Representative data is given in Fig. 14 illustrating the distribution of the max internal pressure coefficient with respect to the wind angle of attack. This variation can be explained as follows; at 0° AoA (flow parallel to eave or ridge), the wind flow direction doesn't see both the edge and overlap openings except those at the gable end. As the angle of rotation increases, however, the infiltration of the wind through the tile opening also increases. The flow begins to see both the edge opening as well as the overlap opening. At 90° AoA, for instance, the wind flow and the openings are face-to-face causing the infiltration of air through the edge opening as well as the overlap openings of the windward side of the roof. This leads to the development of positive internal pressure underneath the tile along the windward side of the roof as shown in Fig. 14.

The opposite direction of the mean external and internal underneath pressures causes reduction in the net pressure that develops on surfaces of the roof tile. The mean underneath pressure on the

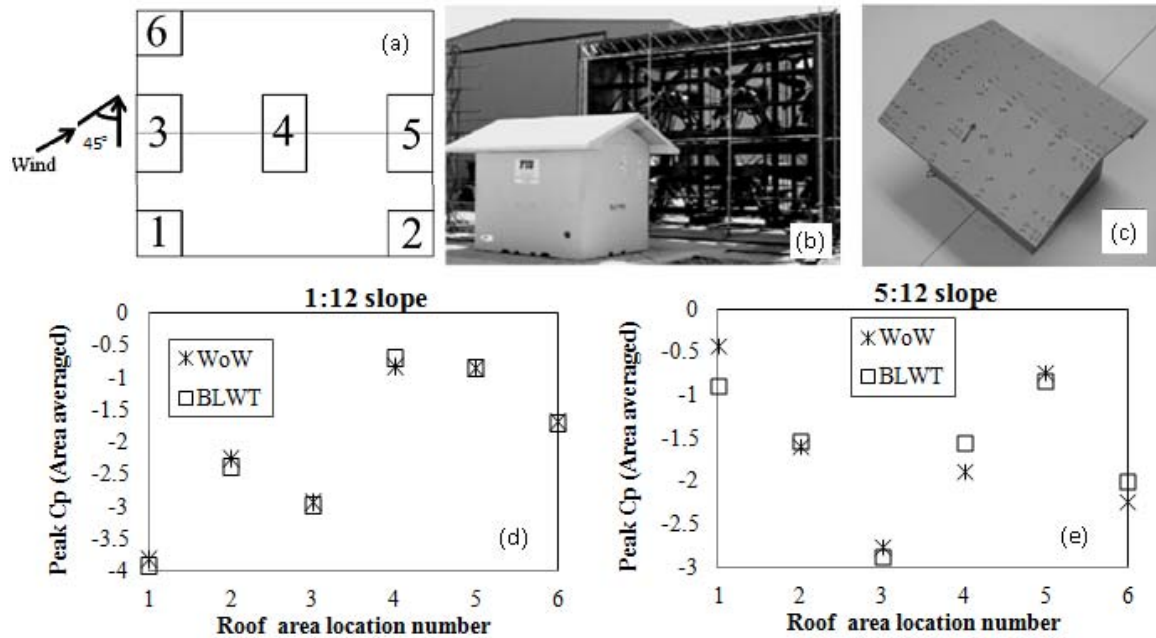


Fig. 17 Comparison of area-averaged peak pressure coefficients for roof area locations (a) from Wind Tunnel (b), and WoW (c), for 1:12 gable roof (d) and 5:12 Gable (e)

windward side was observed to be positive for the three roof slopes tested. The mean external pressures for both the 7:12 and 5:12 roof was also positive. However, it was observed that the 2:12 roof slope experienced a mean suction windward external pressure making the external and underneath pressures in the same direction. As shown in Fig. 15, the combined effect of the windward external and underneath pressure has a reduction effect on the 7:12 and 5:12 roof tiles. However, for the 2:12 roof slope, the combined effect causes an increased suction pressure on the roof tile since both are in the same direction. It was also observed that both the external and underneath pressures on the leeward side were negative for all the tests performed. This has caused a more or less insignificant pressure coefficient on the leeward side of the roof.

The impact of weather blocking on internal pressure underneath tile was also investigated. Even though weather blocking of the roof perimeter using mortar or foam is effective in preventing wind driven rain, it doesn't play a significant role in minimizing the stress on the roof tiles, as a result of the internal pressure underneath tile. As shown in Fig. 16, a comparison between weather blocked and non-weather blocked roof tiles of all types was done. It was observed that the external pressure difference between the two (WB vs NWB) is dominantly insignificant. However, the positive internal pressure underneath the tile when the roof is weather blocked is higher than that when it is non-weather blocked but not that significant to cause drastic change on the net roof pressure. More specifically, the weather blocking produces significant underneath mean pressure on the field tiles on the wind-ward roof thus producing slightly higher net pressures. On the leeward side, reductions in net pressure were observed due to the opposite direction of the internal and external pressures. One should be aware that the weather blocking is used only on the edges of the roof field tile as well as at the intersection of the field and ridge tile. However, the openings which are the sources of internal pressure are all over the roof deck where

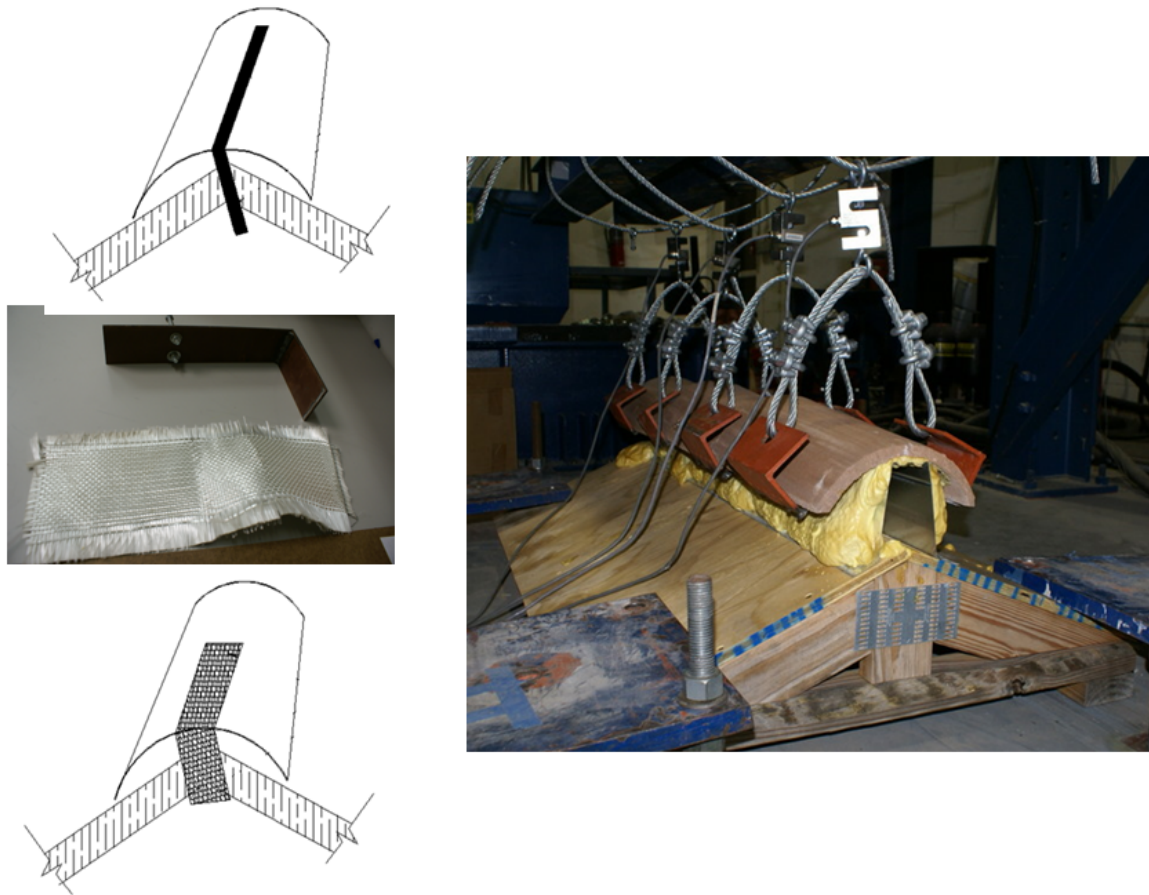


Fig. 18 Metal angle and FRP mitigation techniques

the field tiles are laid (i.e., overlap opening) and the edges (i.e. edge opening). Thus, even though the edges get sealed with weather blocking material, a significant part of the roof is left open causing the intrusion of air underneath the tile.

4. Wall of wind validation

As part of validation of the WoW measurements, a systematic comparison between WoW and typical boundary layer wind tunnel test have been carried out. For this purpose two gable roofs with low- and high-slopes (i.e. 1:12 and 1:15 slopes respectively) without tiles herein after refereed as “bare roof” have been tested at the WoW. In parallel a small-scale (1:20) replica of the same low- and high gable roof models were tested at RWDI Inc. boundary layer wind tunnel in Miramar, Florida under similar flow conditions. Both the WoW and the wind tunnel models are shown in figures as shown in Figs. 17(b) and 17(c), respectively. The area-averaged peak pressures, for each area selected to facilitate equivalent comparisons, as defined in Fig. 16(a), were obtained by instantaneous spatial averaging of the measured point pressure time histories for the five

relevant taps. A reasonable agreement between the wind tunnel and WoW test results for the bare roof models was achieved for all angles of attack. For brevity, the comparative results for 45° wind angle of attack are shown in Fig. 17(d) and 17(e) for the 1:12 and 5:12 slope models, respectively.

4.1 Proposed mitigation

From observation of the experimental analysis, it is shown that the probable failure initiation on a low-rise gable building is found to be the ridge edge at the gable end. A very high suction pressure coefficient was measured in both the barrel type and three-sided ridge tile for the different roof slopes tested. These critical suction pressures could be the causes for the onset of roof tile failure. To address the above stated problems, the following two structural mitigations are suggested: metal angle anchor and FRP fixed to the gable end starting at the ridge tile (Fig. 18). Initial investigation showed that the metal angle mitigation method increased the uplift resistance of the ridge tile by 146%. The methods also keep the aesthetic value of the ridge on the roof.

5. Wall of wind validation

A full scale aerodynamic assessment of field and ridge tiles with variable profiles and slopes was carried out. The external pressures on the roof surface as well as the “internal pressure” underneath the tiles were analyzed in detail to better understand the tile aerodynamics both with weather block and no-weather block conditions. The coefficient of pressure on field and ridge tiles were evaluated for five wind angles of attack (i.e. 0°, 30°, 45°, 75°, 90°). It was observed that the 30° and 45° wind AoA on the edge ridge tile and 0° wind AoA on the corner field tile produced the highest suction pressure for the three roof slopes examined both with weather block and no-weather block conditions. Generally, the coefficients of pressure at the corner and gable end ridges of the roof were significantly high. Relatively, the gable end ridge pressure was obtained to be considerably higher than the corner field tile explaining why failures initiate at these locations as observed in recent post damage assessments. The contribution of internal pressure underneath the roof deck was observed to be significant wherein which it dampens the net suction pressure along the windward side but magnifies that on the leeward side. Aerodynamically, the high profile roof tile performs well over the field, but because of its deep valley, it causes the formation of considerable suction pressure on the ridge tile. The surface geometry of the individual tile was observed to have a significant impact on both the external pressure on the roof surface as well as the internal pressure underneath the roof deck. Please note that these pressures on tiles shall not be used for roof design, rather for design of tile connections/attachments with the roof deck or ridge lines.

Acknowledgments

The financial support from Florida Department of Emergency Management (FDEM) to carry out this project is gratefully acknowledged. The help received from the roofing industry representatives namely Bob Ferrante (Polyfoam Products Inc.), Mike Fulton (O'Hagin Vents), Tim Gabroski (Tim Gabroski Roofing Inc.), Manuel Oyola (Eagle roofing products Florida LLC), Tom Castellanos (East Coast Metals), and Riku Ylipelkonen (Polyfoam Products Inc.) throughout the

project execution both in terms of sharing their experience, installing the tiles on the roofs and donating raw-materials is greatly appreciated. We acknowledge the help received from FIU graduate students – Edward Ledesma, Francis Bain, Asmerom Hagos, and undergraduate research assistants Hugo Altimari. Last but not least we acknowledge the help received from our WoW lab manger Walter Conklin and WoW Research Scientists Roy Liu, James Erwin, and Aly Mousaad Aly. The 6-fan WoW pressure validation study presented here has been conducted by Ruilong Li, PhD candidate at FIU.

References

- ASTM E 1592 (2005), Standard Test Method for Structural Performance of Sheet Metal Roof and Siding Systems by Uniform Static Air Pressure Difference.
- Banks, D. and Meroney, R.N. (2001), "A model of roof-top surface pressures produced by conical vortices: model development", *Wind Struct.*, **4**(3), 227-246.
- Bitsuamlak, G.T., Dagnew, A. and Chowdhury, A. (2009), "Computational assessment of blockage and wind simulator proximity effects for a new full-scale testing facility", *Wind Struct.* (in press)
- Cochran, L.S. and Cermak, J.E. (1992), "Full-and model-scale cladding pressures on the Texas Tech Experimental Building", *J. Wind Eng. Ind. Aerod.*, **43**, 1589-1600.
- Cochran, L.S., Levitan, M.L., Cermak, J.E. and Yeatts, B.B. (1993), "Geometric similitude applied to model and full-scale pressure tap sizes", *Proceedings of the 3rd Asia-Pacific Symp on Wind Eng.*, 917-922, HK.
- Cutter, S.L., Johnson, L.A., Finch, C. and Berry, M. (2007), "The US hurricane coasts: increasingly vulnerable?", *Environment* **49**(7), 8-20.
- Factory Mutual Research Corporation (FM) (1985), "Factory mutual property loss prevention data sheet 1-49 – Perimeter flashing", *Factory Mutual*, Norwood, MA, USA.
- Federal Emergency Management Agency (FEMA) (2004), *Improving school safety*, Risk Management Series design guides, FEMA RMS #424, January, USA.
- Federal Emergency Management Agency (FEMA) (2007), *Improving critical facility safety*, Risk Management Series design guides, FEMA RMS #543, January, USA.
- FM 4470 (1986), Approval Standard for Class 1 Roof Covers.
- Gerhardt, H.J. and Kramer, C. (1992), "Effects of building geometry on roof wind loading", *J. Wind Eng. Ind. Aerod.*, **43**, 1765-1773.
- Hooke, W.H. (2007), "Editor's note", *Nat. Academy Eng.*, **37**(1), 3-4.
- Huang, P., Mirmiran, A., Chowdhury, A.G., Abishdid, C. and Wang, T. (2009), "Performance of roof tiles under simulated hurricane impact", *J. Architec. Eng.- ASCE*, **15**(1), 26-34.
- Institute of Business and Home Safety (IBHS) (1999a), *Metal edge flashing*, Natural Hazard Mitigation Insights, No.10, June, USA.
- Institute of Business and Home Safety (IBHS) (1999b), *Performance of metal buildings in high winds*, Natural Hazard Mitigation Insights, No. 9, January, USA.
- Institute of Business and Home Safety (IBHS) (2009), *Hurricane IKE: nature's force vs structural strength*, Natural Hazard Mitigation Insights, No. 9, January 1999, USA.
- Kawai, H. and Nishimura, G. (1996), "Characteristics of fluctuating suction and conical vortices on a flat roof in oblique flow", *J. Wind Eng. Ind. Aerod.*, **60**, 211-225.
- Kramer, C. and Gerhardt, H.J. (1989), "Wind pressures on roofs of very low and very large industrial buildings", *Proceedings of the 8th Colloq. on Industrial Aerodyn. Part 2. Aachen*, Germany.
- Lin, J.X. and Surry, D. (1998), "The variation of peak loads with tributary area near corners on flat low building roofs", *J. Wind Eng. Ind. Aerod.*, **77-78**, 185-196.
- Lin, J.X., Surry, D. and Tieleman, H.W. (1995), "The distribution of pressure near roof corners of flat roof low buildings", *J. Wind Eng. Ind. Aerod.*, **56**, 235-265.

- Lott, N. and Ross, T. (2006), "Tracking and evaluating U.S. billion dollar weather disasters, 1980-2005", *Forum on Environmental Risk and Impacts on Society: Successes and Challenges*, American Meteorological Society.
- McDonald, J.R. and Smith, T.L. (1990), *Performance of roofing systems in the hurricane Hugo*, Institute for Disaster Research, Texas Tech University, Lubbock, Texas.
- Mehta, K.C. and Levitan, M.L. (1992), "Roof corner pressures measured in the field on a low building", *J. Wind Eng. Ind. Aerod.*, **41**, 181-192.
- Minor, J.E. and Mehta, K.C. (1979), "Wind damage observations and implications", *J. Struct. Division - ASCE*, **11**, 2279-2291.
- Mirmiran, A. (2006), "Hurricane loss reduction for housing in Florida: Section 5- Performance of tile roofs under hurricane impact – Phase I", Retrieved June 10, 2010, from http://www.ihrf.fiu.edu/lwer/docs/Year6_Section5_TileTest_RCMPY6.pdf.
- Mirmiran, A., Wang, T., Abishdid, C., Huang, P., Jiménez, D.L. and Younes, C. (2007), "Hurricane loss reduction for housing in Florida: performance of tile roofs under hurricane impact – Phase II", Retrieved June 11, 2010, http://www.ihrf.fiu.edu/lwer/docs/Year7_Section5_Tiles_RCMPY7.pdf.
- Rappaport, E.N. (2000), "Loss of life in the United States associated with recent tropical cyclones", *Bull. Am. Meteorol. Soc.*, **81**(9), 2065-2074.
- Robertson, A.P., Hoxey, R.P., Rideout, N.M. and Freathy, P. (2007), "Full-scale study of wind loads on roof tiles and felt underlay and comparisons with design data", *Wind Struct.*, **10**(6), 495-510.
- Saathoff, P.J. and Melbourne, W.H. (1989), "The generation of peak pressures in separated /reattaching flows", *J. Wind Eng. Ind. Aerod.*, **32**, 121-134.
- Sparks, P.R., Schiff, S.D. and Reinhold, T.A. (1994), "Wind damage to envelopes of houses and resulting insurance losses", **53**, 145-155.
- Stathopoulos, T. (1987), "Wind pressures on flat roof edges and corners", *Proceedings of the 7th Int. Conf. on Wind Eng. Aachen*, Germany.
- Stathopoulos, T., Baskaran, A. and Goh, P.A. (1990), "Full-scale measurements of wind pressures on flat roof corners", *J. Wind Eng. Ind. Aerod.*, **36**, 1063-1072.
- Tieleman, H.W., Surry, D. and Lin, J.X. (1994), "Characteristics of mean and fluctuating pressure coefficients under corner (delta wing) vortices", *J. Wind Eng. Ind. Aerod.*, **42**, 263-275.
- UL 1897 (2004), Standard for Uplift Tests for Roof Covering Systems.